European Journal of Nuclear Medicine and Molecular Imaging (2019) 46:2392–2397
https://doi.org/10.1007/s00259-019-04408-2

SHORT COMMUNICATION

PET imaging of metabolic changes after neural stem cells and GABA progenitor cells transplantation in a rat model of temporal lobe epilepsy

Ruili Du[1,2,3] · Xiandi Zhu[1,2,3] · Shuang Wu[1,2,3] · Xiaohui Zhang[1,2,3] · Yang He[4] · Kai Zhang[1,2,3] · Xiao He[1,2,3] · Xiaoqun Wang[5] · Yujie Sun[6] · Qiangbin Wang[7] · Hong Zhang[1,2,3] · Mei Tian[1,2,3]

Received: 14 March 2019 / Accepted: 18 June 2019 / Published online: 24 July 2019

Abstract

Purpose Stem cell transplantation is promising for temporal lobe epilepsy (TLE) treatment. This study aimed to use PET imaging for the investigation of dynamic metabolic changes after transplantation of human neural stem cells (NSCs) and human GABA progenitor cells (GPCs) in a rat model of TLE.

Methods ^{18}F-FDG PET imaging, video-electroencephalography (EEG), whole-cell patch-clamp recordings and immunostaining were performed after transplantation of NSCs and GPCs.

Results PET imaging demonstrated that glucose metabolism was gradually improved in the NSCs group, but decreased in GPCs and the control. Video-EEG manifested that seizures were suppressed after NSCs or GPCs transplantation; whole-cell patch-clamp confirmed increased inhibitory response of GPC-derived cells; immunostaining studies verified that the transplanted NSCs and GPCs could survive, migrate and differentiate into mature neuronal subtypes.

Conclusion ^{18}F-FDG PET imaging could be a distinguishing approach for evaluation of dynamic glycolytic metabolic changes after transplantation of NSCs and GPCs in TLE. Whole-cell patch-clamp provides evidence for functional maturation and integration of transplanted stem cells within host circuits.

Keywords Temporal lobe epilepsy (TLE) · Glucose metabolism · Positron emission tomography (PET) · Neural stem cells (NSCs) · GABA progenitor cells (GPCs)

Ruili Du, Xiandi Zhu, Shuang Wu, Xiaohui Zhang, Yang He and Kai Zhang contributed equally to this work.

This article is part of the Topical Collection on Preclinical Imaging

Electronic supplementary material The online version of this article (https://doi.org/10.1007/s00259-019-04408-2) contains supplementary material, which is available to authorized users.

✉ Hong Zhang
hzhang21@zju.edu.cn

✉ Mei Tian
meitian@zju.edu.cn

[1] Department of Nuclear Medicine and PET Center, The Second Hospital of Zhejiang University School of Medicine, 88 Jiefang Road, Hangzhou 310009, Zhejiang, China

[2] Institute of Nuclear Medicine and Molecular Imaging of Zhejiang University, Hangzhou, China

[3] Key Laboratory of Medical Molecular Imaging of Zhejiang Province, Hangzhou, China

[4] Institute of Neuroscience, Zhejiang University School of Medicine, Hangzhou, China

[5] Institute of Biophysics, Chinese Academy of Sciences, Beijing, China

[6] State Key Laboratory of Membrane Biology, Biodynamic Optical Imaging Center (BIOPIC), Peking University School of Life Sciences, Beijing, China

[7] Suzhou Institute of Nano-Tech and Nano-Bionics, Chinese Academy of Sciences, Suzhou, China

Introduction

Temporal lobe epilepsy (TLE) presents in 30% of epileptic patients who do not respond to antiepileptic drugs (AEDs) [1]. Recently, as an alternative to AEDs, cell-based therapy, particularly using neural stem cells (NSCs) or GABA progenitor cells (GPCs), offers an opportunity for eliminating epileptic seizures [2, 3]. Transplanted NSCs and GPCs could differentiate into mature neuronal cells, integrate into host neural circuitry, and thereby promote functional recovery [3, 4]. However, the metabolic changes after stem cell transplantation and its association with therapeutic responses are still poorly understood.

Since [^{18}F] fluorodeoxyglucose positron emission tomography (^{18}F-FDG PET) is the optimal imaging approach for quantitative measurement of glycolytic metabolic changes [5, 6], we hypothesized that ^{18}F-FDG PET should be feasible for evaluation of dynamic metabolic changes after NSCs and GPCs transplantation. Therefore, in the present study we applied ^{18}F-FDG PET, combined with video-electroencephalogram (EEG), whole-cell patch-clamp and immunostaining to investigate the dynamic metabolic and functional changes after transplantation of stem cells for TLE in the rat model.

Materials and methods

Animals

Male adult Sprague-Dawley rats (280–320 g) were randomly assigned into human NSCs-treated, human GPCs-treated, or vehicle-injected as the TLE model control group. To establish the TLE model, the rat was immobilized in a stereotaxic apparatus under 2% isoflurane anesthesia. A double-guide cannula was embedded into the right dorsal hippocampus, then electrodes for recording and reference were implanted into the skull over the right frontal cortex. After one-week recovery, the chemical convulsant, kainic acid (KA; 0.7 μg/5 μl) was unilaterally injected into right hippocampus to induce spontaneous recurrent seizures (SRS). Details are provided in the Supplementary Material.

Stem cell preparation and transplantation

Green fluorescent protein (GFP)-expressed NSCs were derived from a human embryonic stem cell line (chHES 90, National Engineering Research Center of Human Stem Cells, China), and GFP-expressed GPCs were derived from a human embryonic stem cell line (H9 cell line, Wicell, Madison, WI). These cells were prepared as described in the literatures [7, 8]. Four days post KA administration, a total of 1.0×10^6 NSCs or GPCs suspended in a 5 μL volume were stereotactically transplanted into the lesion site (1.0 mm away from the site of KA injection) [4]. An equal volume of vehicle was injected into the same coordinate for the control.

Video-EEG monitoring

Electrographic seizures (amplitude > 2× baseline, frequency > 5 Hz, and duration ≥ 15 s) were monitored by a video-EEG monitoring system (Chengyi, China) 4 h per day for 7 consecutive days. Seizure behaviors were analyzed based on the video-recordings. Behavioral severity was scored between Stage I through V according to the modified Racine scale [9].

PET imaging and image analysis

Rats were kept fasting overnight but had free access to water. PET imaging was performed in the microPET R4 scanner (Siemens Medical Solutions) after injection of 0.5 mCi ^{18}F-FDG via the tail vein. For semiquantitative analysis, regions of interest (ROIs) were defined in the following regions: the right hippocampus including anterior (ventral) and posterior (dorsal) hippocampus (AH and PH), pons was used as a reference region. The regional cerebral metabolism rate (rCMR) of each ROI was calculated as the lesion-to-pons (L/P) ratio [10]. Relative change of rCMR at each time point (t: baseline, Week 1, 3 and 6) compared to the baseline (acquired at 24 h after KA injection) was calculated by the following formula:

$$\text{Relative change of rCMR} = \frac{(\text{L/P})_t}{(\text{L/P})_{baseline}}$$

Whole-cell patch-clamp recordings

Two months after transplantation, whole-cell patch-clamp recordings were processed to monitor electrophysiological properties of GFP$^+$ cells. Action potential (AP) firing and spontaneous excitatory postsynaptic currents (sEPSCs) were recorded with an EPC-10 amplifier (HEKA Elektronik), then 10 μM DNQX (6,7-Dinitroquinoxaline-2,3-dione) was added to block sEPSCs [11]. AP firing reflects that the cell can be stimulated by currents and fire action potential. Individual recordings were analyzed by MiniAnalysis software (Synaptosoft). Details are provided in the Supplementary Material.

Immunostaining

Immunostaining was performed to verify neurogenesis and glucose metabolic activity. Transplanted human NSC and GPC-derived cells were identified by human Nuclei (hNu) staining. NeuN, glial fibrillary acidic protein (GFAP) and glucose transporter-1 (GLUT-1) were applied as mature neuronal,

astrocyte, glucose transporter markers, respectively, and γ-aminobutyric acid (GABA) and neuropeptide Y (NPY) as interneuron markers (details are presented in the Supplementary Material).

Statistical analysis

The data were presented as mean ± s.e.m.; $P < 0.05$ was considered significant. Semiquantitative analysis of PET images was conducted using the AMIDE software package (version 9.2; Stanford University). For comparison of two and multiple groups, Student's t test and ANOVA were respectively performed on Prism 6 software (Graph Pad) to determine possible statistical differences.

Results

Seizure activity

Compared with the control, both NSCs and GPCs groups exhibited a significant reduction in seizure frequency ($P < 0.001$ and $P < 0.01$, respectively) and duration ($P < 0.0001$ and $P < 0.001$, respectively) at week 6 ($n = 8$ per group; Fig. 1a and b). Seizure duration was significantly shortened in the NSCs group at week 3 ($P < 0.01$); no other significant intergroup differences were found at weeks 1 or 3. Vehicle-injected TLE rats showed SRS (Supplementary Fig. 1).

PET imaging findings

PET images showed improved glucose metabolism in the KA-induced epileptic foci (in the right hippocampus) at weeks 3 and 6 for the NSCs group, but not for the GPCs or control ($n = 7$ per group; Fig. 2a). Relative rCMR changes of right hippocampus including both AH and PH were significantly increased for the NSCs group ($P < 0.05$ for each comparison), but not for the GPCs group ($P > 0.05$) at weeks 3 and 6, compared with the control group (Fig. 2b, Supplementary Fig. 2).

Electrophysiological characterization

By using whole-cell patch-clamp recordings, repetitive (Type A, 50%) and single (Type B, 33%) AP firings were observed in transplanted GFP$^+$ GPCs (Fig. 3a left and middle, b), but not in NSCs (Fig. 3a right). Membrane resistance (R_m) was larger in Type A versus Type B cells ($P < 0.05$; Fig. 3c). No significant difference was found in rest membrane potential (RMP) between Type A and B cells (Fig. 3d). GABA-mediated sEPSCs were recorded at −70 mV in voltage-clamp mode from GPCs ($n = 5$; Fig. 3e), and could be completely inhibited by DNQX (Fig. 3f), but showed negative in NSCs ($n = 5$; Fig. 3g).

Immunostaining analysis

Immunostaining of hNu verified that transplanted NSCs and GPCs had migrated from the injection site to the surrounding area within the epileptic hippocampus, co-expressed GLUT1, GABA, NPY, and more mature neuronal marker NeuN (Fig. 4a and b). GFAP$^+$ astrocytes generated from NSCs overlapped with hNu$^+$ cells; however, GFAP expression could be barely seen in GPCs.

Discussion

In the present study, we investigated metabolic and functional changes after transplantation of NSCs and GPCs in a rat model of TLE by using PET imaging combined with video-EEG, whole-cell patch-clamp recordings and

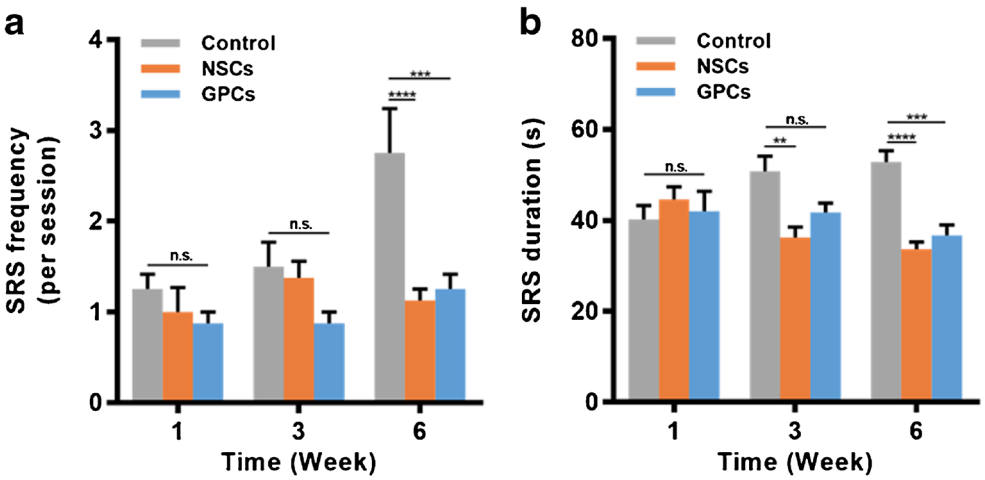

Fig. 1 NSCs and GPCs transplantation inhibited seizure activity in TLE rats. Comparison of spontaneous recurrent seizures (SRS) frequency (**a**) and duration (**b**) in the control, NSCs and GPCs transplantation groups. Data are shown as mean ± s.e.m.; $n = 8$ for each group; n.s. no significant difference, $^{**}P < 0.01$, $^{***}P < 0.001$, $^{****}P < 0.0001$

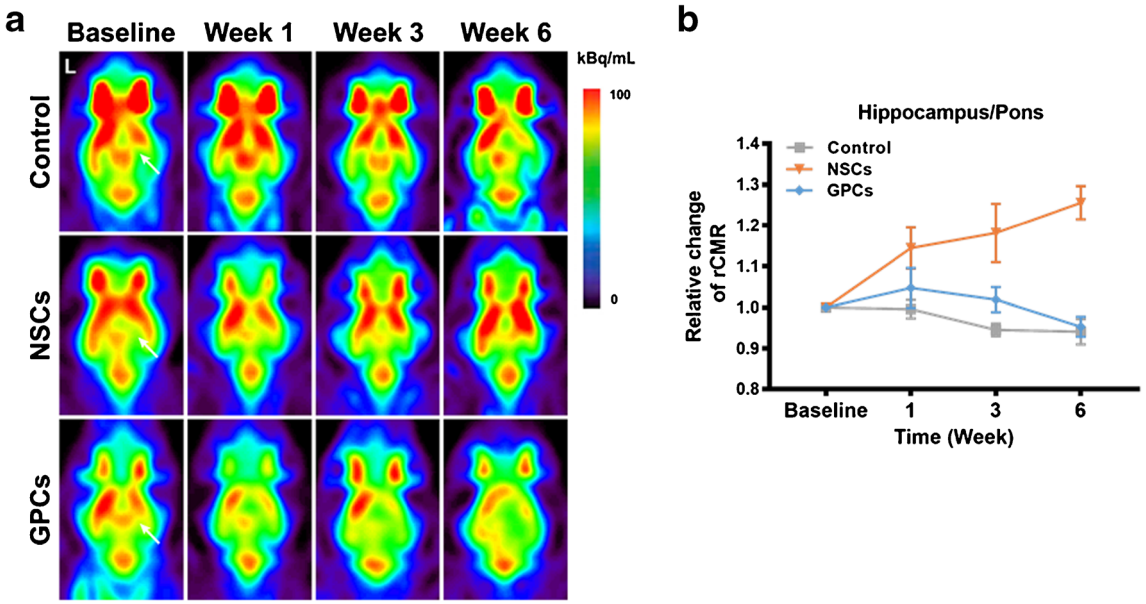

Fig. 2 ^{18}F-FDG PET imaging demonstrated glucose metabolic changes after NSCs and GPCs transplantation in a rat model of TLE. **a** Representative PET images showed gradually recovered glucose metabolism in the NSCs group, but not in the GPCs and the control. The *white arrows* point to the region of hypometabolism. L: left. **b** Relative change of rCMR in each group ($n = 7$ per group). Data are shown as mean ± s.e.m.

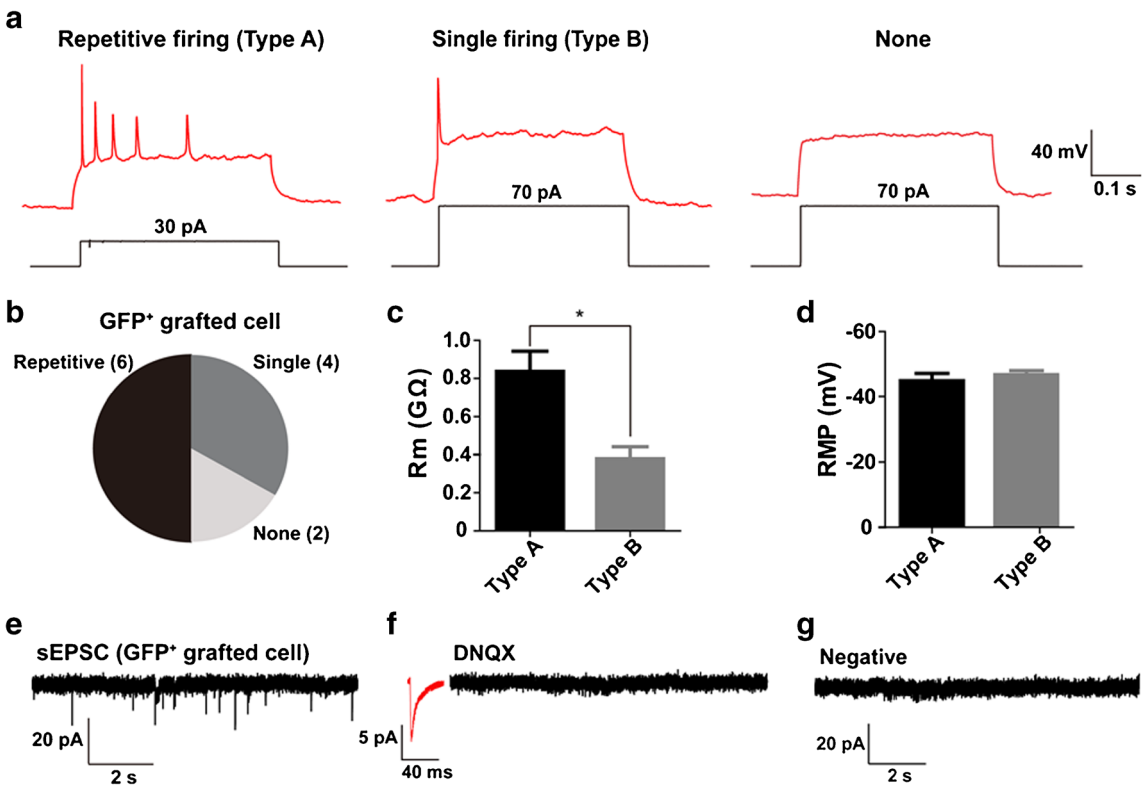

Fig. 3 Electrophysiological properties of the transplanted NSCs and GPCs in the hippocampus. **a** Repetitive (Type A) and single firings (Type B) were recorded in most of GFP$^+$ GPC-derived cells, while no action potential (AP) was recorded in GFP$^+$ NSC-derived cells. **b** A summary pie showing the proportion of different AP firing patterns ($n = 12$ cells). **c–d** Bar graphs showing R_m (**c**) and RMP (**d**) recorded in the Type A or Type B cells. **e–f** Representative sEPSCs recordings from GFP$^+$ GPCs (**e**), inhibited sEPSCs with addition of DNQX (**f**), and negative current from NSCs (**g**). $n = 5$ for each group

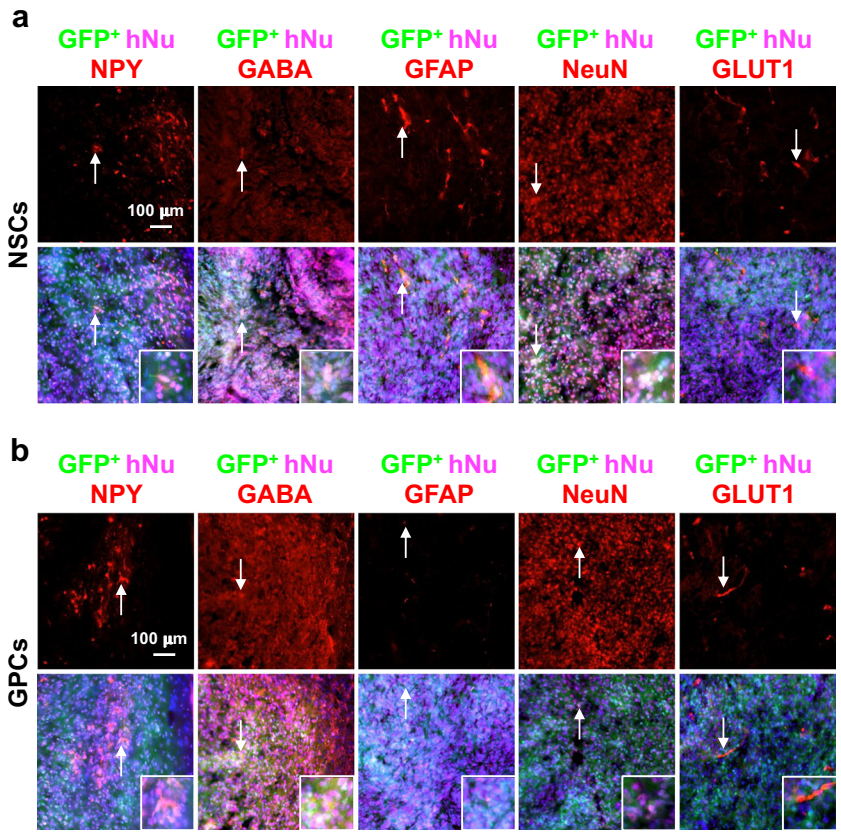

Fig. 4 Immunofluorescent images of transplanted GFP$^+$ cells at 2-month post NSCs and GPCs transplantation. Representative images (200×) of GFP$^+$ (*green*) NSCs (**a**) and GPCs (**b**) co-stained with GLUT1, NeuN, GFAP, GABA, or NPY (*red*); nuclei were counterstained with 4,6-diamino-2-phenylindole (DAPI) (*blue*), and human-Nuclei-specific antibody (hNu) (*pink*). *Arrows* denote examples of merged cells

immunostaining. Seizure frequency and duration were found significantly suppressed in the NSCs and GPCs groups compared with the control group. Relative change of rCMR was significantly increased in the NSCs but decreased in the GPCs group. To our knowledge, this is the first PET imaging study on direct comparison between NSCs and GPCs for TLE, which was verified by video-EEG, whole-cell patch-clamp recordings and immunostaining.

PET imaging revealed that hippocampal glucose metabolism was significantly improved in the NSCs group, suggesting NSCs transplantation prevented interictal hypometabolism in the KA-induced epileptic foci. However, local glucose consumption was not recovered in the GPCs group, which was consistent with the relatively weaker suppression of seizure activity monitored by video-EEG. The hypometabolism in the control was likely ascribed to the factors such as cell loss, diaschisis, increased interictal glutamate level, or mitochondrial dysfunction [12] (further discussions are presented in the Supplementary Material). In addition, we found that the EEG patterns of these KA-treated rats were characterized by an initial convulsive status epilepticus, followed by a latent phase, until the appearance of SRS. Repetitive and single firings were recorded in the GPC-derived cells, and GABA-mediated sEPSCs could be inhibited completely by DNQX, an AMPA/kainate-type glutamate receptor antagonist [11], which implied that transplanted GPCs had integrated into host neural circuitry, differentiated into functional GABAergic interneurons and received excitatory synaptic inputs from host glutamatergic neurons.

Whole-cell patch-clamp recordings confirmed transplanted GPCs could specifically differentiate into GABAergic interneurons, which in turn re-established neurotransmitter glutamate and GABA homeostasis by releasing GABA. The transplanted GABAergic interneurons could release inhibitory neurotransmitter GABA and increase inhibitory synaptic responses in host hippocampal neurons, therefore exerting antiepileptic effects [13]. In addition, the inhibitory process might not be able to lead to a significantly increased metabolism, while the excitatory process can lead to a significantly increased metabolism [14]. Therefore, the GPCs group had a significant improvement in seizures but did not have an FDG improvement. And vise versa, the negative patch-clamp recordings for NSCs indicated the relatively immature NSCs might need a prolonged period to reach full electrophysiological maturation, compared with GPCs [15]. Such differences between GPCs and NSCs in differentiation phases may also account for the discrepancy of glucose metabolism. Furthermore, our immunostaining studies indicated that transplanted NSCs and GPCs could disperse from the original injection site, integrate into host hippocampal

networks, and differentiate toward GABAergic interneurons to regulate the excitatory-inhibitory neuronal balance.

Conclusion

^{18}F-FDG PET imaging could be a distinguishing approach for evaluation of dynamic glycolytic metabolic changes after transplantation of NSCs and GPCs in TLE. Whole-cell patch-clamp provides evidence for functional maturation and integration of transplanted stem cells within host circuits.

Acknowledgements We thank Qianyun Liu (Hopstem Biotechnology LLC) for technical support on immunostaining, and Prof. Linghui Zeng (Department of Pharmacology, School of Medicine, Zhejiang University City College) for patch-clamp data analysis.

Funding This study was sponsored by the National Key Research and Development Program of China (2016YFA0100900), National Natural Science Foundation of China (NSFC) (81761148029, 81725009, 81571711, 81425015), and Zhejiang University K.P. Chao's High Technology Development Foundation.

Compliance with ethical standards

Conflict of interest The authors declare no conflicts of interest.

Ethical approval All experiments were performed following protocols of the Institutional Animal Care and Use Committee (IACUC) of Zhejiang University School of Medicine (Protocol No. #ZJU2015-068-02), under the regulations of the Association for Assessment and Accreditation of Laboratory Animal Care International (AAALAC International) and National Research Council's Guide for the Care and Use of Laboratory Animals.

References

1. Chen Z, Brodie MJ, Liew D, Kwan P. Treatment outcomes in patients with newly diagnosed epilepsy treated with established and new antiepileptic drugs: a 30-year longitudinal cohort study. JAMA Neurol. 2018;75(3):279–86.
2. Waldau B, Hattiangady B, Kuruba R, Shetty AK. Medial ganglionic eminence-derived neural stem cell grafts ease spontaneous seizures and restore GDNF expression in a rat model of chronic temporal lobe epilepsy. Stem Cells. 2010;28:1153–64.
3. Upadhya D, Hattiangady B, Castro OW, Shuai B, Kodali M, Attaluri S, et al. Human induced pluripotent stem cell-derived MGE cell grafting after status epilepticus attenuates chronic epilepsy and comorbidities via synaptic integration. Proc Natl Acad Sci USA. 2019;116(1):287–96.
4. Miltiadous P, Kouroupi G, Stamatakis A, Koutsoudaki PN, Matsas R, Stylianopoulou F. Subventricular zone-derived neural stem cell grafts protect against hippocampal degeneration and restore cognitive function in the mouse following intrahippocampal kainic acid administration. Stem Cells Transl Med. 2013;2(3):185–98.
5. Zhu Y, Feng J, Wu S, Hou H, Ji J, Zhang K, et al. Glucose metabolic profile by visual assessment combined with statistical parametric mapping analysis in pediatric patients with epilepsy. J Nucl Med. 2017;58(8):1293–9.
6. Ding Y, Zhu Y, Jiang B, Zhou Y, Jin B, Hou H, et al. (18)F-FDG PET and high-resolution MRI co-registration for pre-surgical evaluation of patients with conventional MRI-negative refractory extratemporal lobe epilepsy. Eur J Nucl Med Mol Imaging. 2018;45(9):1567–72.
7. Xu JC, Fan J, Wang X, Eacker SM, Kam TI, Chen L, et al. Cultured networks of excitatory projection neurons and inhibitory interneurons for studying human cortical neurotoxicity. Sci Transl Med. 2016;8(333):333ra48.
8. Liu Y, Liu H, Sauvey C, Yao L, Zarnowska ED, Zhang S-C. Directed differentiation of forebrain GABA interneurons from human pluripotent stem cells. Nat Protoc. 2013;8(9):1670–9.
9. Racine RJ. Modification of seizure activity by electrical stimulation. II. Motor seizure. Electroencephalogr Clin Neurophysiol. 1972;32(3):281–94.
10. Kornblum HI, Araujo DM, Annala AJ, Tatsukawa KJ, Phelps ME, Cherry SR. In vivo imaging of neuronal activation and plasticity in the rat brain by high resolution positron emission tomography (microPET). Nat Biotechnol. 2000;18(6):655–60.
11. Baraban SC, Southwell DG, Estrada RC, Jones DL, Sebe JY, Alfaro-Cervello C, et al. Reduction of seizures by transplantation of cortical GABAergic interneuron precursors into Kv1.1 mutant mice. Proc Natl Acad Sci USA. 2009;106(36):15472–7.
12. Van Paesschen W, Dupont P, Sunaert S, Goffin K, Van Laere K. The use of SPECT and PET in routine clinical practice in epilepsy. Curr Opin Neurol. 2007;20(2):194–202.
13. Cunningham M, Cho JH, Leung A, Savvidis G, Ahn S, Moon M, et al. hPSC-derived maturing GABAergic interneurons ameliorate seizures and abnormal behavior in epileptic mice. Cell Stem Cell. 2014;15(5):559–73.
14. Waldvogel D, van Gelderen P, Muellbacher W, Ziemann U, Immisch I, Hallett M. The relative metabolic demand of inhibition and excitation. Nature. 2000;406(6799):995–8.
15. Lu P, Ceto S, Wang Y, Graham L, Wu D, Kumamaru H, et al. Prolonged human neural stem cell maturation supports recovery in injured rodent CNS. J Clin Investig. 2017;127(9):3287–99.